

Performance of the Beam Position Monitor System of the Final Focus Test Beam *

S. SMITH, P. TENENBAUM , AND S.H. WILLIAMS

Stanford Linear Accelerator Center, Stanford University, Stanford, CA 94309 USA

Abstract

The Beam Position Monitor (BPM) system for the Final Focus Test Beam (FFTB) at SLAC is designed to meet challenging specifications in the areas of single-pulse resolution, *ab initio* installation accuracy, and time-stability of BPM electrical centroids. We review the tolerances on these quantities and the technical choices made to achieve same, and detail the results of several studies of the actual performance of the system. These results are then related to the BPM system requirements for a future high-energy e^+e^- linear collider.

Submitted to *Nuclear Instruments and Methods A*

*Work supported by Department of Energy contract DE-AC03-76SF00515.

1 Introduction

The Final Focus Test Beam (FFTB) is a beamline designed to demonstrate the demagnification necessary at the interaction point of a future high-energy e^+e^- linear collider [1]. In order to achieve and maintain the large demagnification of the incoming beam ($1/M > 300$), it is necessary to control the orbit through the quadrupole and sextupole magnets with high precision. Consequently, the Beam Position Monitor (BPM) system must perform with a high degree of accuracy, precision, and stability relative to BPM systems previously installed at SLAC.

In addition to the requirements imposed by the goals of the FFTB, the BPM system's performance was measured against the specifications of the Next Linear Collider's main BPM system, the quadrupole ("Q") BPMs. Table 1 details the specifications of the two systems.

The design of the FFTB BPM system is described in detail elsewhere [2]. The system consists of a stripline-style pickup installed inside the bore of a quadrupole magnet, connected by RG-223 cables to signal processing modules installed in air-conditioned buildings; typical lengths of cable-runs are 200 feet. The electronics used to process the stripline signals consists of a 2-channel preamplifier module connected to a 2-channel, 16-bit Track-and-Hold module ("NiTnH"), which digitizes the peak signal from the preamplifier and transmits it to the control system computer network. A single preamplifier and NiTnH is used to process either the top and bottom striplines or the left and right striplines; conversion to position within the aperture of the beam pipe is via the formula:

$$x_1, y_1 = \frac{a S_1 - S_2}{2 S_1 + S_2}, \quad (1)$$

where S_1 and S_2 are the digitized signals from either left and right or top and bottom striplines, and a is the aperture radius of the BPM. Because the FFTB has a sufficient number of BPM channels to read out both planes of each BPM on each pulse, a higher-order correction to Equation 1 was added to the readout software:

$$x_2, y_2 = x_1, y_1 \left[1 + \frac{x_1^2 + y_1^2}{a^2} \right]. \quad (2)$$

This correction allowed the BPMs to report large beam oscillations with greater accuracy. The NiTnH can be operated in self-triggering or externally-triggered modes.

In addition to the readout electronics, the full system includes a Test Pulse Generator (TPG) which allows calibration of each channel on demand. The calibration algorithm is as follows: the NiTnH is triggered in the absence of beam to measure the pedestals, P_1 and P_2 , of each channel; then the TPG injects a pulse into the preamplifier which is split equally between the two channels, and the NiTnH is triggered, allowing the control system to measure the gain of the test pulse through each channel. The standard calibration software measures the gain of each channel at 5 test pulse amplitudes, 10 pulses per amplitude, and computes a mean gain ratio, G , between the two channels. This gain ratio is stored in the main computer and used to compensate measured beam positions. The formula for converting a “raw” 16-bit word from a NiTnH into a value for use in position computations is:

$$S_1 = V_1 - P_1, \quad S_2 = G(V_2 - P_2), \quad (3)$$

where V_1 and V_2 are the raw digital words from each of the two channels.

The total FFTB system includes 33 standard stripline units, each 457.2 mm long with a bore radius of 11.5 mm; 1 oversized standard unit, with a bore of 17.5 mm; and 5 large-bore units, each with a radius of 26 mm.

Between 1992 and 1997 the FFTB BPM system was fabricated, installed, tested, and used to produce beams as small as 70 nm in RMS vertical size [3]. In the following we describe the measured performance of the BPM system in the areas of accuracy, precision, and stability over time.

2 Fiducialization

The vast majority of standard FFTB BPM stripline units are installed in the inner bore of quadrupoles. Prior to final installation on the beamline itself, each quadrupole-stripline combination was fiducialized in order to determine the position of the quadrupole magnetic center and the position of the BPM electrical center rela-

tive to the mechanical center of the magnet [4, 5]. A schematic of the fiducialization test stand is shown in Figure 1.

The central feature of the fiducialization system was a wire of diameter 35 microns and mass/length of 0.022 grams/meter; a length of 1.6 meters of wire was stretched through the aperture of the combined quadrupole/BPM assembly and held taut by a 150 gram weight over a jewelled pulley. The wire was connected at either end to mechanical actuators made by the Newport Corporation [6], each capable of moving in horizontal and vertical directions with a resolution of approximately 1 micron. In order to determine the position of the wire with respect to an external coordinate system, a microscope outfitted with tooling balls was employed: the wire would be brought into focus on the microscope, and a Mitutoyo Coordinate Measuring Machine (CMM) [7] would be used to determine the position of the tooling balls; since the focal point of the microscope had previously been fiducialized to the microscope's tooling fixture, the position of the wire could be determined by repeating the procedure above at two points along the length of the wire. In order to fix the longitudinal positions of the measurement for all quadrupole/BPM units tested, the wire was contained throughout its length by a copper pipe with two windows through which the microscope could be employed. This method of determining the wire position was found to have a repeatability of 2.5-5 microns.

After installation on the test stand, each quadrupole was connected to power and cooling-water lines, and a current of 165 amperes was used to establish magnetic excitation. Once thermal equilibrium had been established (usually 3-4 hours after initial powering of the magnet), the quadrupole was fiducialized in the external coordinate system by mechanically vibrating the wire at its resonant frequency of 81 Hz and observing the spectrum of the EMF-induced current on the wire. The wire was moved inside the bore of the quadrupole via the translation stages until the EMF at the vibration frequency was nulled, indicating that the wire was at the magnetic center of the quadrupole. This procedure was performed separately in horizontal and vertical planes. At that time the vibration drivers were switched off and a pulse generator was connected to the wire. The pulse generator caused a current pulse

to flow down the wire, which simulated the excitation of an electron beam on the striplines. Each stripline was then read out by a specialized testing apparatus similar to the BPM processing electronics described above. In order to eliminate biases in the measurement due to differing channel gains, a single channel was used to read out each strip in turn.

The stripline excitations were measured as a function of wire position within the aperture. This allowed determination of the *ab initio* positioning accuracy of the BPM center relative to the quadrupole magnetic center, and also allowed direct measurement of the scaling between the actual wire position and the position as reported by the BPM.

The wire position was moved through a grid from -3.0 mm to +3.0 mm in x and y, relative to the measured magnetic center of the quadrupole, in 1.0 mm steps; in all, 49 measurements were made of the signals at each of the 4 striplines. A global fit of all the data for a given BPM was then performed:

$$\begin{aligned} x_{\text{wire}} &= A \left(\frac{V_{\text{left}} - V_{\text{right}}}{V_{\text{left}} + V_{\text{right}}} \right) - x_0 + B \cdot x_{\text{wire}} \cdot (x_{\text{wire}}^2 + y_{\text{wire}}^2), \\ y_{\text{wire}} &= A \left(\frac{V_{\text{top}} - V_{\text{bottom}}}{V_{\text{top}} + V_{\text{bottom}}} \right) - y_0 + B \cdot y_{\text{wire}} \cdot (x_{\text{wire}}^2 + y_{\text{wire}}^2), \end{aligned} \quad (4)$$

where parameters A , B , x_0 , y_0 were the quantities to be fitted and V_{top} , V_{bottom} , V_{left} , V_{right} are the detected voltages of each of the 4 striplines with the wire at a given position $(x_{\text{wire}}, y_{\text{wire}})$. Sources of error in Equation 4 include scale factors and other errors in the positioning of the wire, and relatively poor signal-to-noise ratio on the detection of the stripline signals. To account for these errors, an error on the wire position of 20 microns at each point was assumed.

A total of 26 BPMs were fiducialized using the procedure shown above. Figure 2 shows the measured offsets between quadrupole and BPM centers as measured on the fiducialization test stand. The maximum offset measured was 400 microns in the horizontal and 200 microns in the vertical. With the exception of one extreme value in each plane, the RMS spread of values was 64 microns in the horizontal and 62 microns in the vertical; the average offset in the horizontal is -3 microns and in the vertical is 34 microns. The resolution of the technique was estimated to be 25

microns.

Figure 3 shows the fitted values of A in each BPM tested. From Equation 1, we expect the value of A to be equal to half the BPM radius, or 5.75 mm; the value of A predicted by POISSON simulations is close to 5.6 mm. The fitted value of A averages 5.28 mm, with an RMS variation over the ensemble of 4%. Equations 1 and 2 show that the value of B should always be equal to $1/(4A^2)$, and this was found to be the case for all BPMs fiducialized in this manner.

After fiducialization, the quadrupole/BPM assemblies were transported to the FFTB housing and installed.

3 Precision

The resolution of the BPM system is measured at the beginning of every FFTB run by measuring the position of a large number of beam pulses (typically 100) on BPMs which are at nearly-equal betatron phases. Typically these BPMs are the BPMs in the Chromatic Correction Sections (CCSX and CCSY) surrounding the sextupoles, where the beam is large and the divergence is small. The measurements are performed in a special “tune-up” optics, in which the betatron functions at the sextupoles and the final quadrupole lenses is reduced relative to the small-spot optics, since reducing the betatron functions eliminates the chromaticity of the beamline and reduces the pulse-to-pulse jitter, which improves the convergence of some beam-based tuning algorithms. In this configuration the betatron functions at the CCSY sextupoles is still on the order of 400 meters, resulting in a pulse-to-pulse jitter of 40 microns and an angular jitter of 0.25 microradians RMS. The beam positions in two BPMs at this location, separated by less than 1 meter, should be almost perfectly correlated, and the RMS of the incoherent beam position measurements should provide a direct measure of the BPM precision.

Figure 4 shows the measured beam positions in the downstream BPM of one such CCSY pair, as a function of the position in the upstream BPM. As expected, the two signals are strongly correlated: the RMS distance from a fitted line through the

data is 1.69 microns. Assuming that each BPM contributes equally to this error, the resolution of each BPM is given by the fit error divided by $\sqrt{2}$, or 1.13 microns. The data for Figure 4 was taken with a bunch charge of 7.0×10^9 electrons; a resolution of 1.13 microns at this charge implies a resolution of 0.79 microns at the full charge of 1×10^{10} .

In addition to the precision measurement described above, an additional test involving all of the BPMs was performed. In this measurement, all of the BPMs were read out over several hundred pulses; a least-squares fit to the data was performed, and the RMS fit residual at each BPM evaluated. The results of this measurement are consistent with the resolution figure derived above.

Early experiments with the FFTB BPMs indicated that the striplines are quite sensitive to beam haloes at large amplitudes (“spray”): under poor halo conditions the resolutions can be degraded by over an order of magnitude, due to electrons impacting the striplines. One step in the initial setup for an FFTB run is to use the BPM resolution as a diagnostic on the positioning of adjustable beam-halo collimators in the end of the SLAC linac: the collimators are moved into a position which roughly optimizes the performance of the first few BPMs in the system, which typically requires the jaws be roughly 3 mm from the beam core.

4 Accuracy

The description of fiducialization above details the procedure by which the offset between the BPM electrical center and the quadrupole magnetic center is determined. However, this procedure does not determine offsets due to cabling mismatches, mechanical shifting of the BPM in the quadrupole bore, or gradual changes of the offset with time. In order to measure the BPM offsets directly at the beginning of each major FFTB run, a beam-based alignment procedure is performed. The procedure is described in detail elsewhere [8]: each quad in the beamline is changed in focusing strength from nominal value K_q to $K_q - dK_q$ and $K_q + dK_q$; the resulting deflection

in a downstream BPM is given by:

$$dx_{\text{BPM}} = dx_{\text{Quad}} R_{12}^{\text{Quad} \rightarrow \text{BPM}} \Delta K_q, \quad (5)$$

where ΔK_q is the change in quadrupole focusing strength, dx_{BPM} is the change in the downstream BPM reading, dx_{Quad} is the distance from the beam to the magnetic center of the quadrupole which is being scanned in strength, and $R_{12}^{\text{Quad} \rightarrow \text{BPM}}$ is the R_{12} transfer matrix element from the downstream face of the quad to the BPM. The fractional change in each quadrupole strength is limited by the induced deflection for reasonably misaligned quadrupoles, and by the resulting change in beam size in downstream apertures. At each quadrupole strength all the BPMs in the FFTB are read out for 8-10 pulses, and a global fit is performed for three to six quadrupole misalignments via MINUIT[9]. Once the quadrupole misalignments are known, the BPM offsets can be determined by adding the magnet misalignment to the measured beam position in that magnet's BPM.

While the beam-based alignment procedure was performed many times between 1994 and 1997, the final, optimized algorithm was only used twice: in March of 1995 and May of 1997. We shall discuss results from these periods solely in this report. In each run a total of 30 quadrupoles were aligned, but our discussion will concentrate on a subset of these, 21 in all, for which the alignment could be performed using solely the standard-geometry BPM described above. Furthermore, two out of the 21 BPMs will not be considered in all aspects of the following discussion: the second BPM in the beamline had poor performance in the 1997 run, due to beam conditions which will be described below, and thus comparisons between 1995 and 1997 will exclude this unit; the first BPM in the beamline is installed in a quad which suffered a leak of its cooling water between 1995 and 1997, requiring that the quad be disassembled and reassembled, and thus comparisons between 1995 and 1997 will also neglect this BPM.

Figure 5 shows the fitted horizontal offsets of 19 FFTB BPMs in the 1995 run (horizontal axis) and the 1997 run (vertical axis). The weighted average position offset from 1995 data is 1 micron, with a standard deviation of 90 microns; from the

1997 data the weighted average is 71 microns, with standard deviation of 123 microns. The RMS difference between the two data sets is 70 microns.

In early 1994 beam-based alignment measurements, 4 of the BPMs in Figure 5 were found to have horizontal offsets in excess of half a millimeter. This was believed due to improper masking of synchrotron radiation from the horizontal bending magnets in the CCSX and CCSY, since each of the 4 BPMs was immediately downstream of a bend magnet. The measured offsets were measured at that time and a software correction added; the data in Figure 5 is after this subtraction, as noted on the figure.

Figure 6 shows the fitted vertical offsets of 19 FFTB BPMs in the 1995 run and the 1997 run. Weighted-average offsets in 1995 were 43 microns, with standard deviation 100 microns, and in 1997 were 34 microns with standard deviation 112 microns. The RMS difference between 1995 and 1997 data is 25 microns.

Several factors may contribute to the changes in measured BPM offsets from 1995 to 1997. First, the beam conditions in 1995 were substantially better than those in 1997: the 1995 run came at the conclusion of a prolonged run of the Stanford Linear Collider (SLC), resulting in excellent emittances and relatively low backgrounds due to adjustment of the linac collimators; the 1997 experiment preceded an SLC run, and emittances and collimator adjustment were relatively poor. Consequently, both beam halo impacting BPMs and relatively intense haloes being distorted by the quadrupole strength scans caused problems in 1997 which were not present in 1995. Figure 7 shows that the fit resolution in 1997 was systematically poorer than in 1995, supporting this hypothesis. In addition, the quads were found to be relatively well-aligned in 1995, resulting in small oscillations of the beam as quads are scanned. This makes the 1995 experiment closer to a classical “nulling” test, and the 1995 results more reliable than those in 1997. Finally, seasonal and/or long-term drift of parts of the installation may be involved.

Figure 8 compares the vertical offsets of the BPMs measured in the fiducialization test stand with those measured in the 1995 beam-based alignment experiment. While a correlation is present, the RMS difference in the two measurements is 70 microns, much larger than the differences between the 1995 and 1997 beam-based

alignment runs. This could indicate that a substantial component of the offsets measured with the beam are due to cabling, post-fiducialization shifting of the BPMs in the quadrupole bores, or processing electronics; or it could indicate unexplored systematic differences between the two methods.

5 Stability

Two experiments were performed which investigated the stability of the FFTB BPM system over time. In one test, the calibration procedure for BPM electronics described above was performed once per hour and the variation in time of pedestals and gain ratios was observed. In the other test, a trio of beam position monitors separated by drift spaces was read out once every 6 minutes throughout the one-week FFTB run in December of 1997. Both investigations are described below.

5.1 Electronics Calibration Test

The online calibration procedure described above generates 3 calibration constants for each BPM processor: two pedestals, P_1 and P_2 , and a gain ratio between the two channels, G . If the calibration constants change with time by an amount dP_1 , dP_2 , and dG , respectively, then in the limit where $dG \ll G$, $P_1, P_2, dP_1, dP_2 \ll V_1, V_2$, and $G \approx 1$, the change in measured position due to an uncompensated drift in the calibration is given, to lowest order, by:

$$\Delta x_{\text{BPM}} = \frac{a}{4} \left[\frac{GdP_2 - dP_1}{G(V_2 - P_2)} - dG \right]. \quad (6)$$

During a 1 week FFTB run in late December of 1997, the online calibration procedure was executed once per hour on a total of 123 FFTB-style BPM processors. Of these, 82 are installed in the FFTB and 41 are installed in the Next Linear Collider Test Accelerator, a self-contained X-band test linac not in operation at the time [10]. In addition to measuring the pedestals and gain ratios of the BPM processors, the calibration system does a set of checks on the quality of the results and flags processors which do not pass the checks. Processors can be flagged if they fail to respond to cali-

bration triggers, return zeroes for all calibration parameters, demonstrate excessively nonlinear or noisy gain ratios, or return gain ratios which are substantially different from 1.0. Figure 9 shows the number of calibrations per processor which passed the system's quality check. Seven processors in FFTB showed an excessive number of failures and were excluded from the analysis, leaving 116 processors.

In order to determine the approximate resolution of the system, a test was performed in which the calibration routine was executed repeatedly as rapidly as possible, resulting in 30 calibrations in 5 minutes. The RMS variation in pedestals from this test was found to be approximately 2 counts, while the RMS variation in gain ratios was found to be approximately 2×10^{-4} . These are taken to be the resolution limits of the measurement.

The pedestal drift was determined by computing $GP_2 - P_1$ for each processor on each calibration, and computing an RMS of this quantity for each processor. Figure 10 shows the distribution of RMS pedestal drifts over 1 week. The average was 2.2 counts, and no unit had an RMS greater than 4.05 counts. Since the typical signal level from an FFTB BPM stripline with the beam centered and a bunch charge of 7×10^9 electrons is 12,000 counts, an RMS drift of 2.2 counts corresponds to a centering drift of 0.5 microns.

A similar analysis of the gain ratio was performed: for each processor the value of G was stored once per hour, and a mean and RMS computed. Figure 11 shows the distribution of gain ratio RMS values. While 68% of all processors showed RMS gain variations of 1.2×10^{-3} or less, the distribution includes a long tail out to a variation of 4×10^{-2} . A gain ratio drift of 1.2×10^{-3} results in a centering drift of 3.5 microns, while a drift of 4×10^{-2} results in a drift of 115 microns.

One environmental factor which has a strong effect on the BPM processors is the ambient temperature. The SLAC control system maintains a record of all CAMAC crate temperatures which is updated once every 6 minutes. Figure 12 shows the distribution of the normalized correlation coefficient between crate temperature and gain ratio for the processors: note that more than half the units have an 80% or greater correlation between the two. Figure 13 shows the RMS in the residual gain

ratio, i.e., the RMS of $G_i - T_i m_i$, where G_i is the measured gain ratio, T_i is the measured crate temperature, and m_i is the slope of a line fitted to the temperature-gain ratio data. Figure 13 shows the expected RMS gain ratio variation assuming that the equipment hut temperatures can be controlled with arbitrary precision and that the gain ratio depends linearly on the temperature. In this case 68% of the processors have an RMS drift of less than 5.2×10^{-4} . While the tail is truncated in this case, some processors with extremely large variations are still apparent. Finally, Figure 14 shows the distribution of RMS gain ratios expected if the temperature variation is reduced to 1° Centigrade RMS. In this case, 68% of processors have a gain variation of less than 7.9×10^{-4} , corresponding to a centering drift of 2.3 microns in FFTB.

5.2 Three-BPM Test

Consider three BPMs separated only by drift spaces, in which the distance from the first BPM to the second is given by L_2 and between the first and third is given by L_3 . If the 3 BPMs have position offsets given by dx_1, dx_2, dx_3 and position readings given by x_1, x_2, x_3 , then for a beam pulse with arbitrary incoming position and angle the relationship between the offsets and the beam position readings should be given by:

$$D_x \equiv x_3 - \frac{L_3}{L_2} x_2 + \left(\frac{L_3}{L_2} - 1 \right) x_1 = dx_3 - \frac{L_3}{L_2} dx_2 + \left(\frac{L_3}{L_2} - 1 \right) dx_1 \quad (7)$$

A similar equation describes the relationship between BPM readings and BPM offsets in the vertical plane. During the December 1997 FFTB run a software “watchdog” was used to record the values of D_x (and the equivalent vertical function D_y) once every six minutes throughout the run. Each reading averaged over four pulses, and therefore the expected statistical error in D_x and D_y is 0.5 microns. The three BPMs are near the waists in the middle of the Beta Exchanger, where the betatron functions are reasonably small (tens of meters rather than thousands), and therefore neither BPM nonlinearities nor spray are expected to be an issue. The December 1997 FFTB run came after several months of SLC operations, and consequently the emittances were quite good ($\gamma\epsilon_x \approx 30\text{mm} \cdot \text{mrad}$, $\gamma\epsilon_y \approx 1.3\text{mm} \cdot \text{mrad}$).

Figure 15 shows the values of D_x , D_y , and the bunch charge as a function of

time, after eliminating data points in which the beam was not present or the data presented a discontinuous “jump” (indicating a rogue beam pulse hitting an aperture upstream). The data from the horizontal plane has a sudden discontinuous step of 150 microns, and consequently the standard deviation of D_x is 89 microns. In the vertical no step is seen and the RMS is 23 microns. Note that the vertical data is strongly correlated to the bunch charge (normalized correlation coefficient of 0.85). This most likely arises from different saturation behaviors of the processors involved, a phenomenon observed during initial tests of the BPM system [2]. Figure 16 shows the value of D_y as a function of time after subtracting the linear dependence on bunch charge; RMS drift in the value is reduced to 12 microns.

During the December 1997 FFTB run the BPM online calibration was operating every hour, but the resulting changes in calibration were not being applied to data taken online. Figure 17 shows the expected change in the value of D_y due to drifts in the processors. When these drifts are subtracted from D_y , the RMS is reduced to 11.2 microns.

Finally, a correlation was observed between the value of D_y and the beam position measured at the first BPM. This is likely due to the aforementioned BPM scale factor issue. The three BPMs used in this test were never tested on the fiducialization test stand because they are not part of a quadrupole installation; however, the fiducialization of quadrupole BPMs indicated variations of several percent in the scale factors of the different BPMs. Because the vertical betatron function is largest at the first of the 3 BPMs used in this experiment, and because that BPM enters Equation 7 with a scale factor of $L_3/L_2 - 1 \approx 2.5$, it is not unexpected that a scale factor error would cause a correlation between the reading of the first BPM and the value of D_y . Figure 18 shows the value of D_y when correlations to temperature, bunch charge, and position in the first BPM are eliminated. The RMS drift of D_y in Figure 18 is 8.9 microns, with 12-hour periods (such as the one indicated on day 5 of the run) during which the variation is as small as 3 microns. Correlations between Figure 18 and the second and third BPM raw readings are negligible.

If we assume that the drifts in Figure 18 are due to uncorrelated drifts in the

offsets of the 3 BPMs, the single-BPM figure of merit can be determined by dividing the RMS in Figure 18 by $\sqrt{(L_3/L_2)^2 + (L_3/L_2 - 1)^2 + 1}$. For this set of BPMs, this factor has a value of 4.5225, resulting in a single-BPM figure of merit of 2.7 microns. A smaller study of FFTB BPM performance, in which the calibration test and the three-BPM test were performed at different times, predicted that the single-BPM figure of merit was approximately 2.9 microns [11].

6 Conclusions

We have studied the accuracy, resolution, and time-stability of the beam position monitors installed in the Final Focus Test Beam. The single-bunch resolution of the system was found to meet the desired 1 micron specification even at bunch charges somewhat lower than the 1×10^{10} indicated in the design, although the resolution is strongly tied to beam-quality parameters as well. The installation accuracy was on the order of 250-300 microns for all BPMs; the beam-based measurements of installation accuracy are consistent within 70 microns in the horizontal and 25 microns in the vertical over a time of 26 months between measurements, and are consistent with bench test measurements within approximately 70 microns. The BPM processing electronics contributes 3.5 microns of slow offset drifts which are primarily due to temperature variations in the processor crates. The BPM center position is strongly correlated with the bunch charge, possibly because of nonlinearities in the BPM processing electronics which are not properly accounted for in the calibration algorithm. An additional 2.7 microns of offset drift seem to arise from sources outside of the electronics, though this has not been as well studied and statistics are much poorer.

While the BPM system for future linear colliders will necessarily be somewhat different from that used in the FFTB (primarily due to the bunch trains expected in linear colliders), the performance of the FFTB system gives cause for some optimism. The single-pulse resolution desired for a future linear collider has been amply demonstrated in FFTB, as has the *a priori* installation accuracy. The time-stability demonstrated is not quite good enough for a high-luminosity linear collider, but since

the linear collider is likely to have smaller BPM apertures some of the sources of drift will scale down to less problematic dimensions. For example, the expected BPM radius in the linac of a future linear collider is closer to 5 mm than the 11.5 mm used in FFTB[12]; consequently, the 7.9×10^{-4} gain ratio drift measured in the FFTB BPM processors would result in only 1 micron of observed offset drift. A somewhat different calibration philosophy (in which BPMs are calibrated continually rather than on demand) or technique (for example, sending a pulse down one stripline and measuring the response of the nearest two others) may also improve the situation.

The most clearly identified shortcoming of the present state of the art is the bench test facility. Optimally the linear collider's fiducialization test stand should test a quadrupole and its BPM, the actual electronics modules which will read out that BPM, and even the cables which will join them, if possible. The signal used for BPM fiducialization should be as perfect an imitation of the beam as possible. Such a system could potentially be used to obtain a better understanding of the causes of long-term BPM offset drift, which in turn could be applied to correcting same.

Acknowledgements

The authors would like to thank G. Fischer, H. Hayano, Jeff Rifkin, Vernon Smith, and Lee Ann Yasukawa.

References

- [1] K. Oide, Design of Optics for the Final Focus Test Beam at SLAC, in: F. Bennett and J. Kopta, eds., *Proceedings PAC-89* (Chicago, 1989) 1319-1321.
- [2] H. Hayano *et. al.*, High Resolution BPM for FFTB, *Nucl. Instrum. Meth.* **A320** (1992) 47-52.
- [3] V. Balakin *et. al.*, Focusing of Submicron Beams for TeV Scale e^+e^- Linear Colliders, *Phys. Rev. Lett.* **74** (1995) 2479-2482.
- [4] G.E. Fischer *et. al.*, Precision Fiducialization of Transport Components, in: H. Henke, H. Homeyer, and Ch. Petit-Jean-Genaz, eds., *Proceedings EPAC-92* (Berlin, 1992) 138-140.
- [5] P. Tenenbaum *et. al.*, Precision Measurement of Transport Components, in S.T. Corneliussen, ed., *Proceedings PAC-93* (Washington, D.C., 1993) 2838-2840.
- [6] Newport PM 500 Series, Newport Corporation.
- [7] Mitutoyo C806 Coordinate Measuring Machine.
- [8] P. Tenenbaum *et. al.*, Beam-Based Alignment of the Final Focus Test Beam, in: *Proceedings IWAA-95* (Tsukuba, 1995) 393-402.
- [9] M. Roos, 'MINUIT', A System for Function Minimization and Analysis of the Parameter Errors and Correlations, in: *Comput. Phys. Commun.* **10** (1975) 343-367.
- [10] R.D. Ruth *et. al.*, A Test Accelerator for the Next Linear Collider, in: *Proceedings LC-92* (Garmisch, 1992) 155-206.
- [11] P. Tenenbaum, Studies of Beam Position Monitor Stability, to be published in: R. Hettel, S. Smith, J. Masek, eds., *Proceedings of the 1998 Beam Instrumentation Workshop*, AIP Conference Proceedings **451** (Stanford: 1998).

- [12] The NLC Design Group, *Zeroth-Order Design Report for the Next Linear Collider* (SLAC, 1996) 351.

Table Captions

1. System requirements for FFTB and NLC “Q” BPMs.

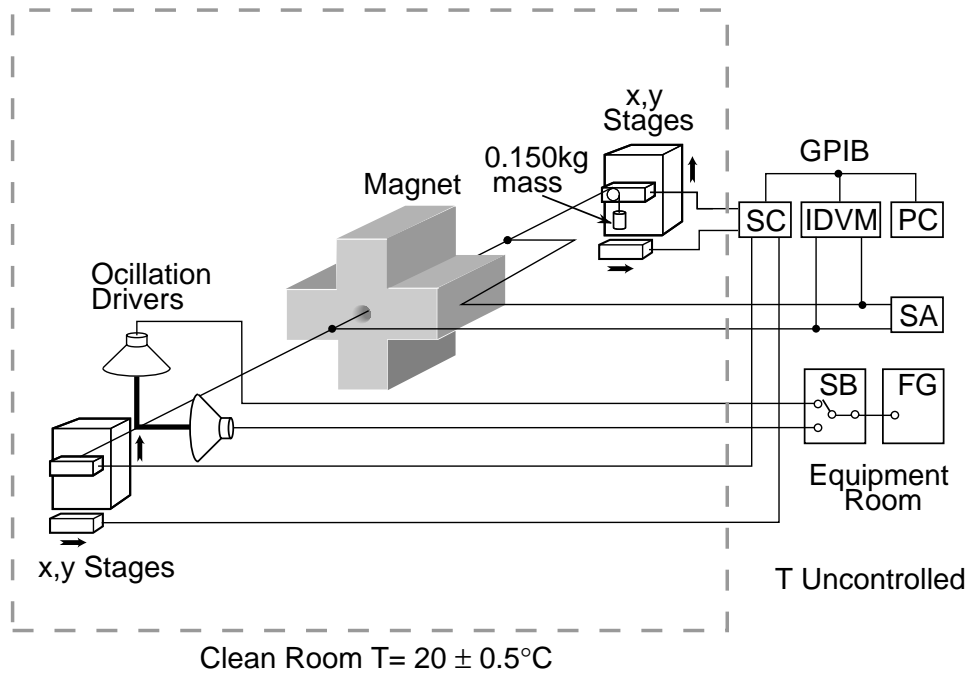
Figure Captions

1. Apparatus used to fiducialize BPMs mounted inside the bore of FFTB quadrupoles. The stepper-motor controllers (SC) are controlled by a PC via GPIB interface, while the spectrum analyzer (SA), function generator (FG), and oscillation-driver switch box (SB) are controlled by the operator. The integrating digital voltmeter (IDVM) is not used in this application.
2. Measured offsets between quadrupole and BPM center for 26 units tested.
3. Measured values of $a/2$ for fiducialized BPMs. The dotted line is at the average value of 5.28 mm.
4. Beam vertical position read on neighboring BPMs at a local β_y^{\max} point for 136 pulses. The RMS fit error is 1.69 microns, implying a resolution of 1.13 microns. The measurement was made at a bunch charge of 7.0×10^9 electrons.
5. Horizontal BPM offsets of 19 FFTB BPMs determined by quad-shunting technique: measurements from March of 1995 (horizontal axis) and May of 1997 (vertical axis) are shown. The RMS difference between the two datasets is 70 microns. Four BPMs have large offsets due to synchrotron radiation, measured in 1994, subtracted; these are indicated by circles.
6. Vertical BPM offsets of 19 FFTB BPMs determined by quad shunting technique in March of 1995 (horizontal axis) and May of 1997 (vertical axis). The RMS difference between the two sets of measurements is 25 microns.
7. Resolution of BPM offsets determined by quad shunting technique in March 1995 (light) and May 1997 (dark). The later experiment was performed under substantially degraded beam conditions, resulting in poorer resolution.
8. Comparison of BPM offsets measured with the quad-shunting technique in March 1995 (horizontal axis) with those measured during fiducialization (vertical axis). The RMS difference between the two measurements is 70 microns.

9. Number of calibrations which passed the calibration software's quality check during a 1 week period. A total of 138 calibrations were performed at hourly intervals. The seven processors which failed to calibrate properly more than 50% of the time are excluded from further analyses.
10. Distribution of RMS variation of $GP_2 - P_1$ over 116 BPM processors. Typical variations were on the order of 2 counts, and no unit experienced a variation greater than 4.05 counts.
11. Distribution of RMS variations of gain ratio for 116 BPM processors. Figure (a) shows all 116, while (b) shows the distribution excluding 7 units with very poor performance and is on a correspondingly tighter scale.
12. Distribution of the normalized correlation coefficient between temperature and gain ratio for 116 BPM processors.
13. Distribution of RMS gain ratio variations after eliminating the linear temperature correlation. Seven processors with poor performance are not shown.
14. Expected distribution of RMS gain ratio variations if temperature variation is limited to $\pm 1^\circ$ Centigrade RMS.
15. Values of D_x , D_y and the bunch charge from December 1997 FFTB run.
16. D_y after suppression of linear dependence on bunch charge. The RMS variation is 12 microns.
17. Contribution to D_y from slow drifts in the electronics, as measured by the online calibration software.
18. D_y after eliminating linear dependence on bunch charge, electronics calibration, and incoming beam position. RMS variation is reduced to 8.9 microns.

Attribute	FFTB BPMs	NLC “Q” BPMs
Max. bunch charge	1×10^{10}	1×10^{10}
Resolution at Max. charge	1 micron	1 micron
<i>Ab initio</i> accuracy	500 microns	200 microns
long-term (> 24hr) center stability	1 micron	1 micron

Table 1.



5-93

7390A1

Figure 1.

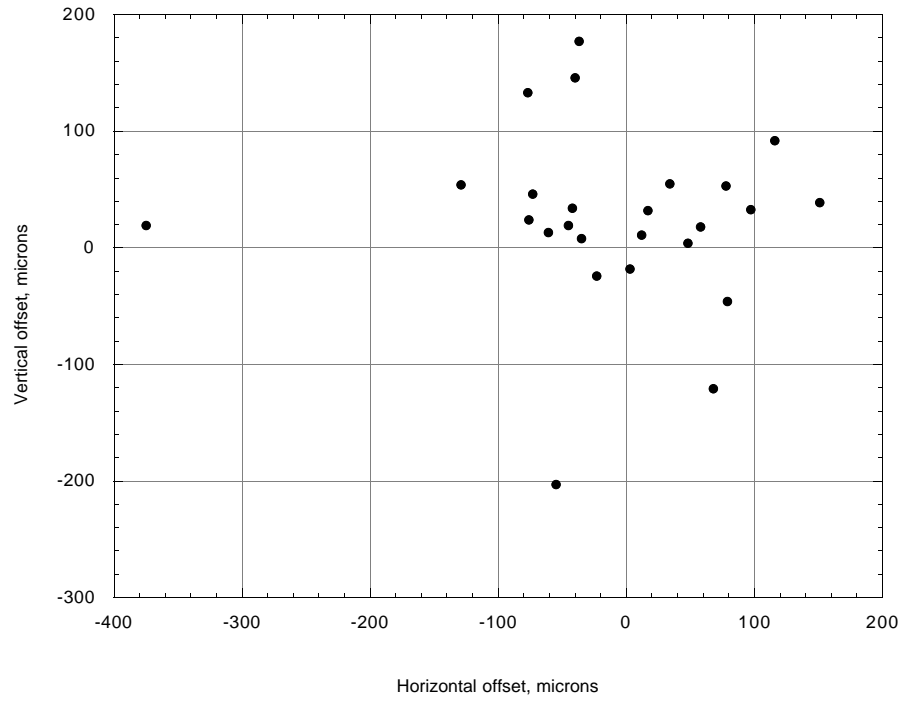


Figure 2.

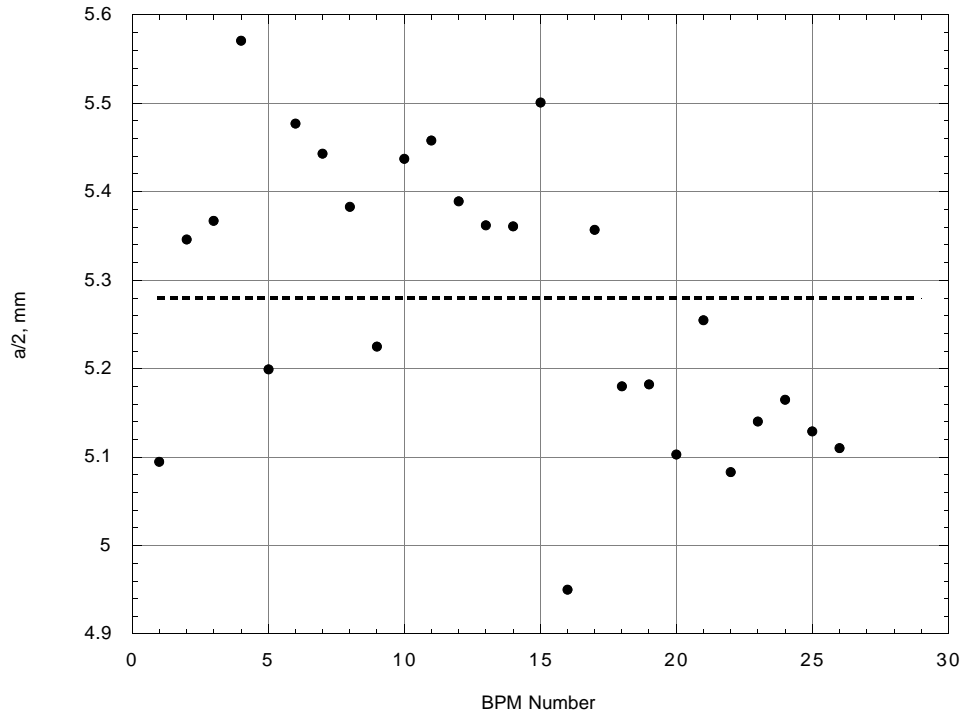


Figure 3.

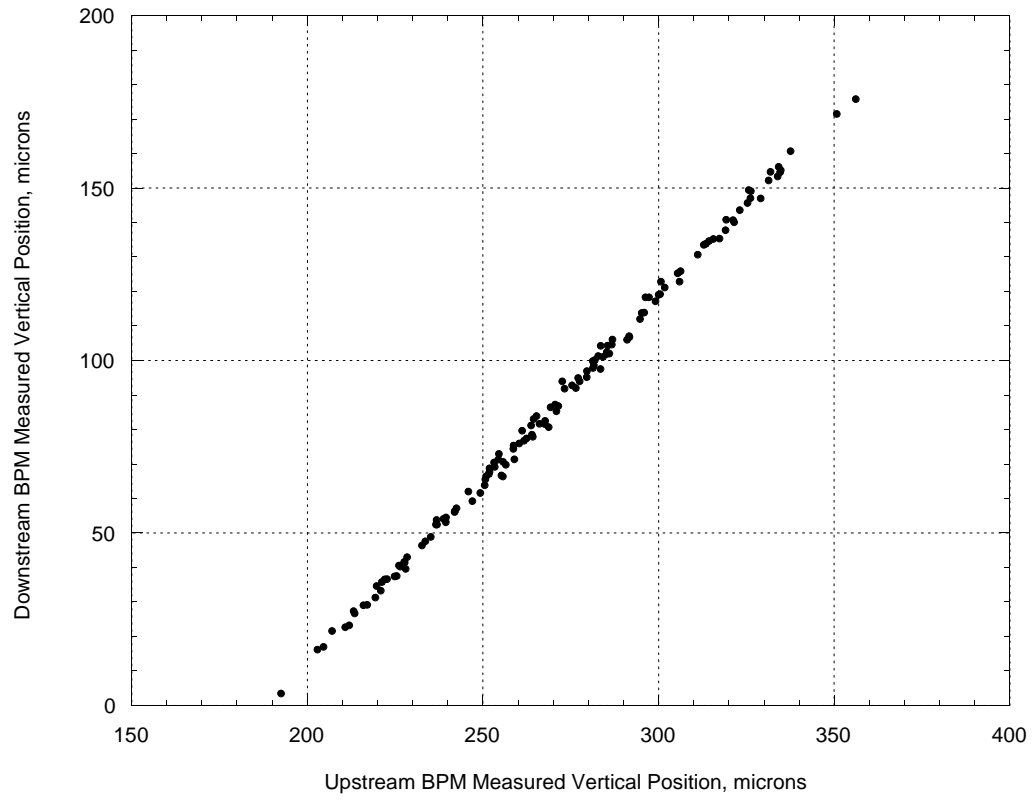


Figure 4.

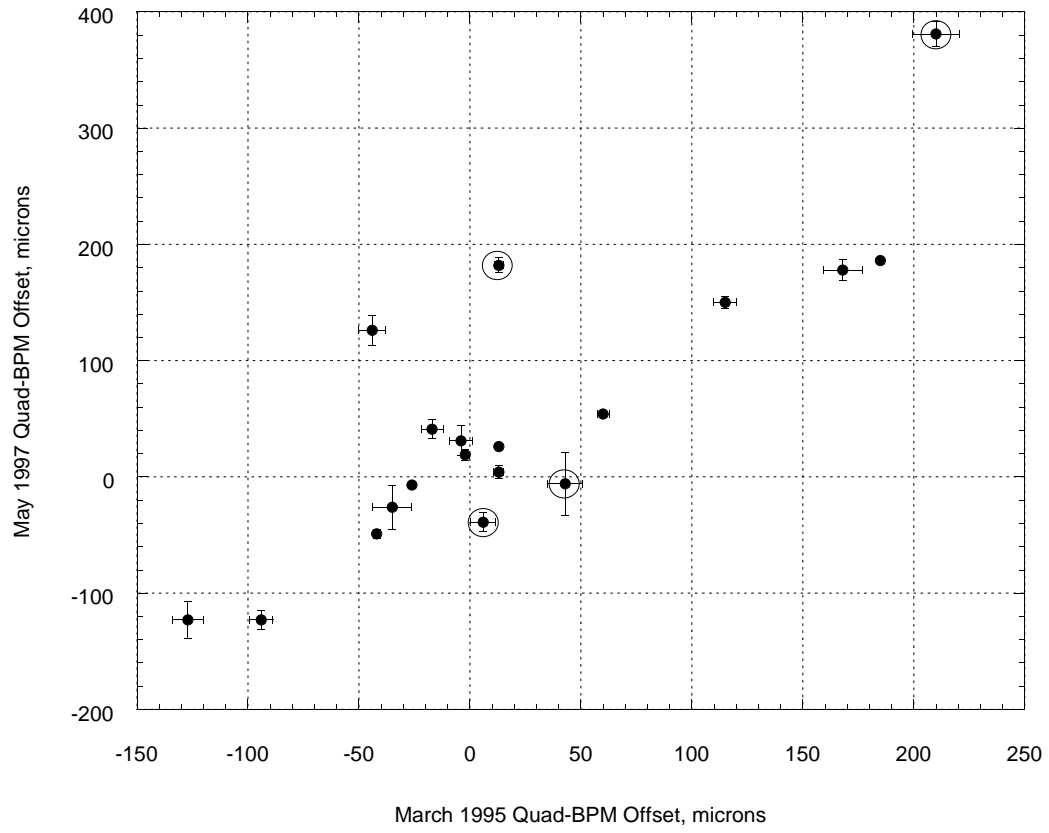


Figure 5.

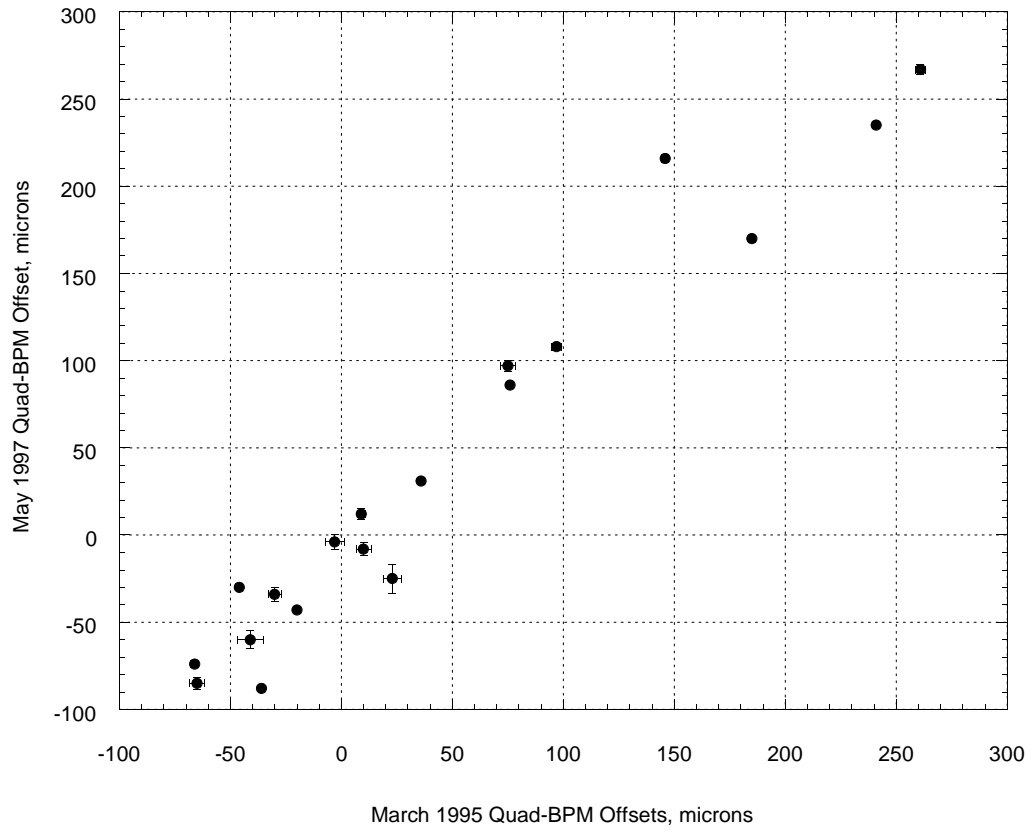


Figure 6.

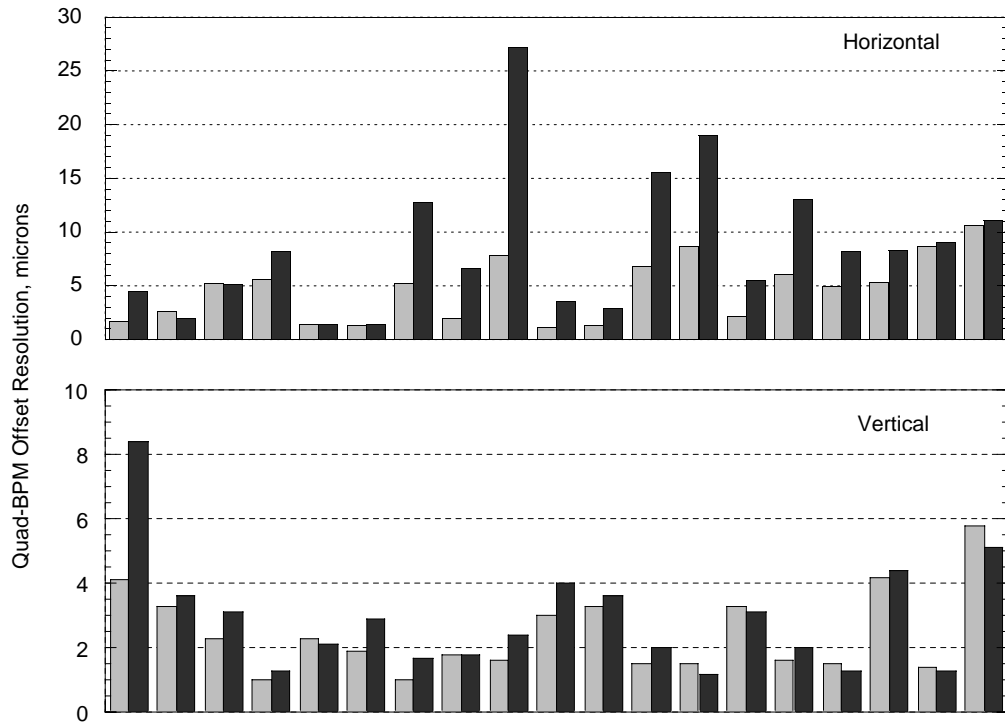


Figure 7.

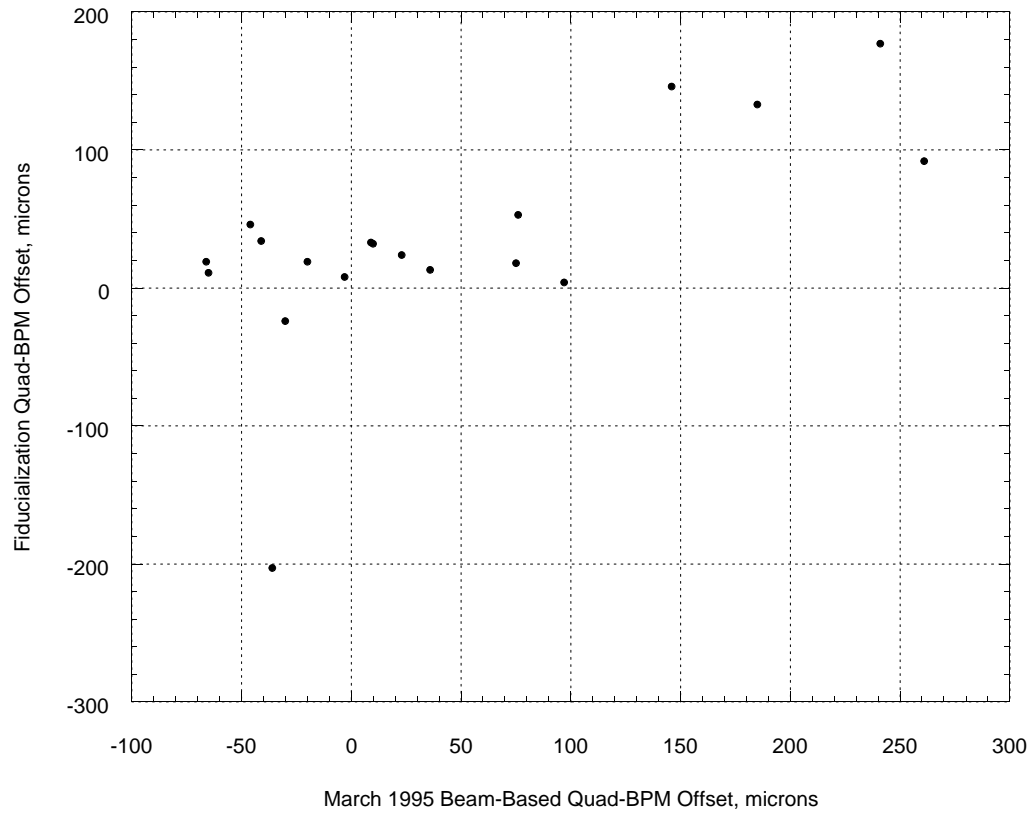


Figure 8.

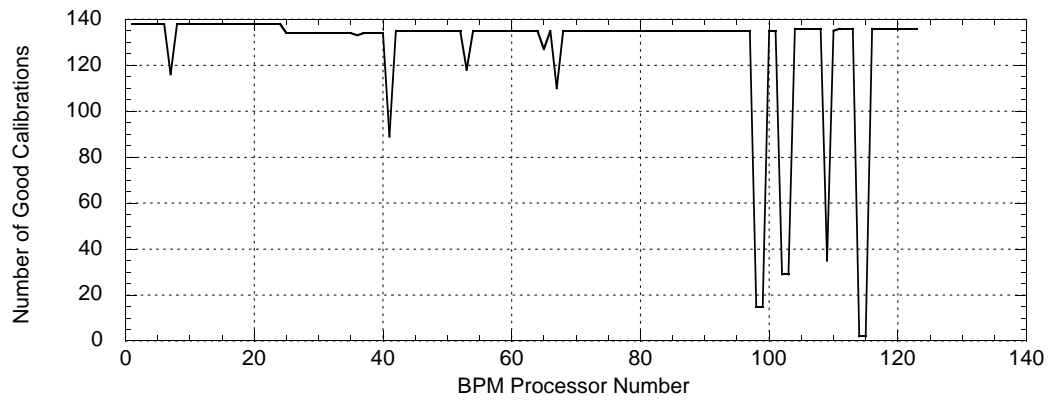


Figure 9.

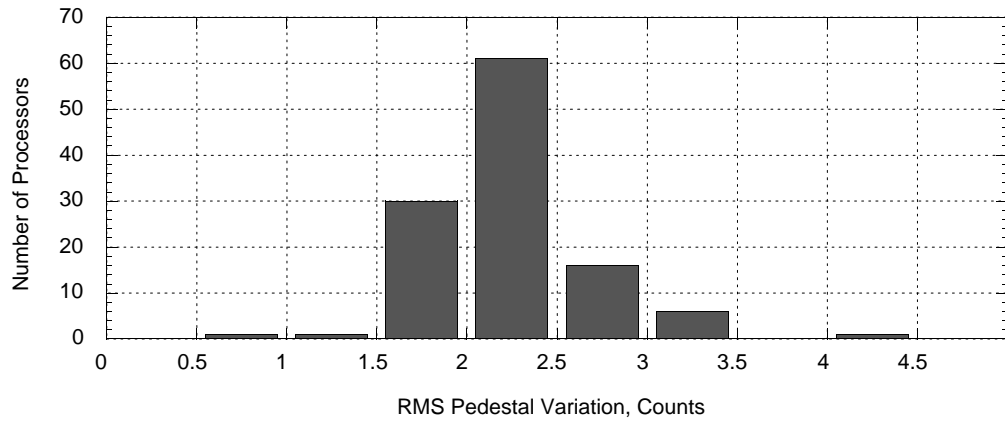


Figure 10.

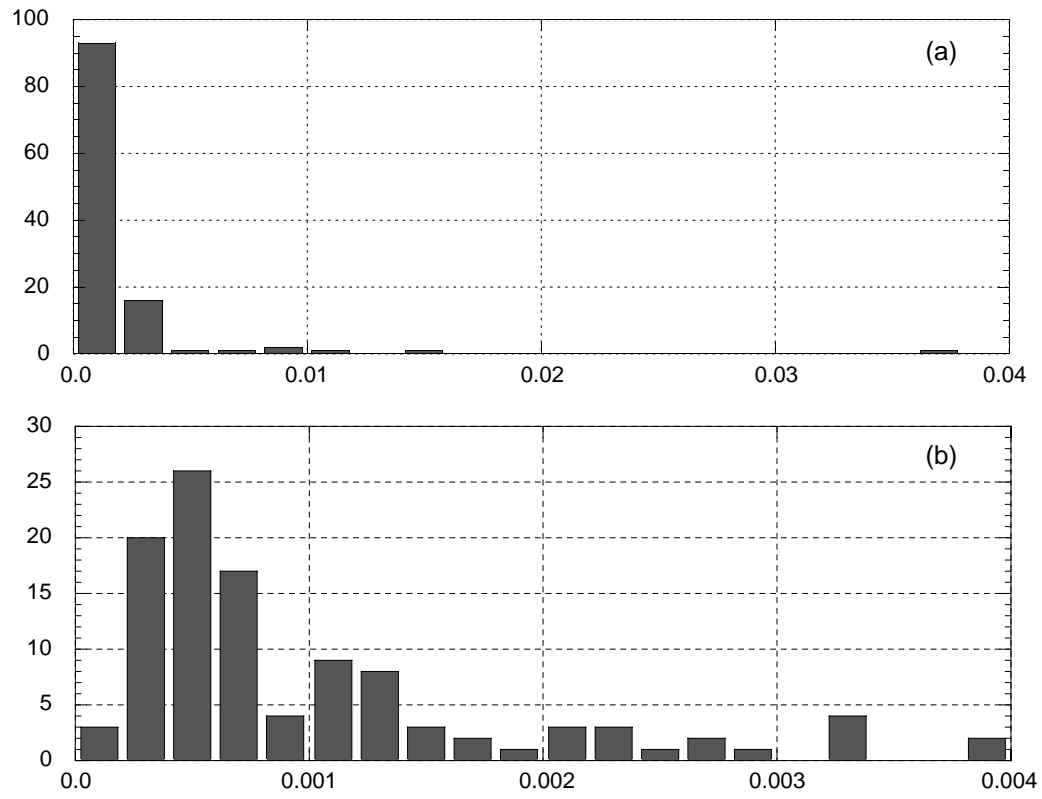


Figure 11.

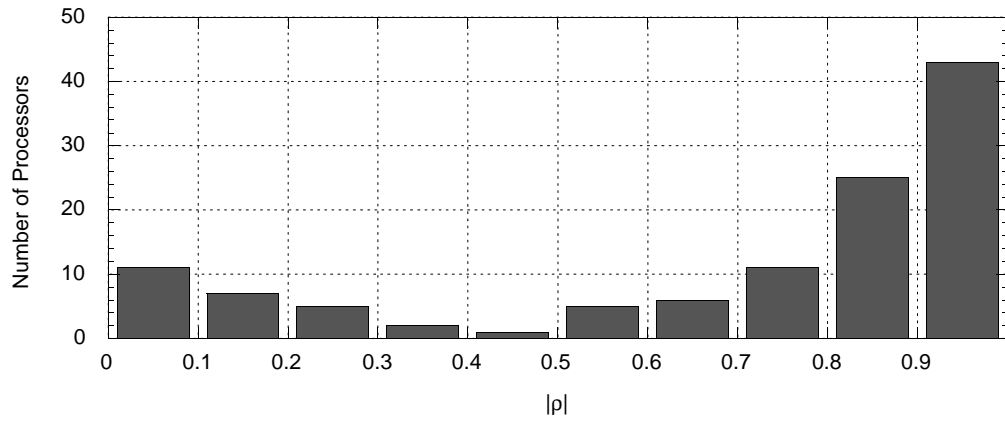


Figure 12.

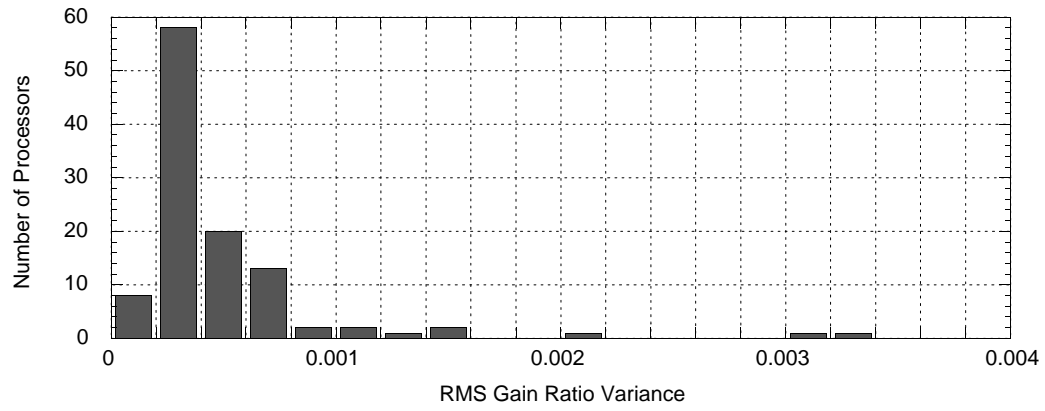


Figure 13.

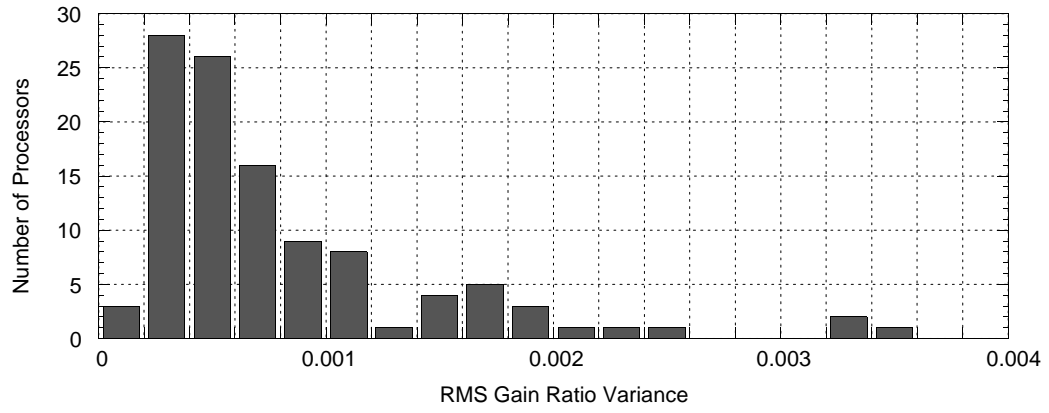


Figure 14.

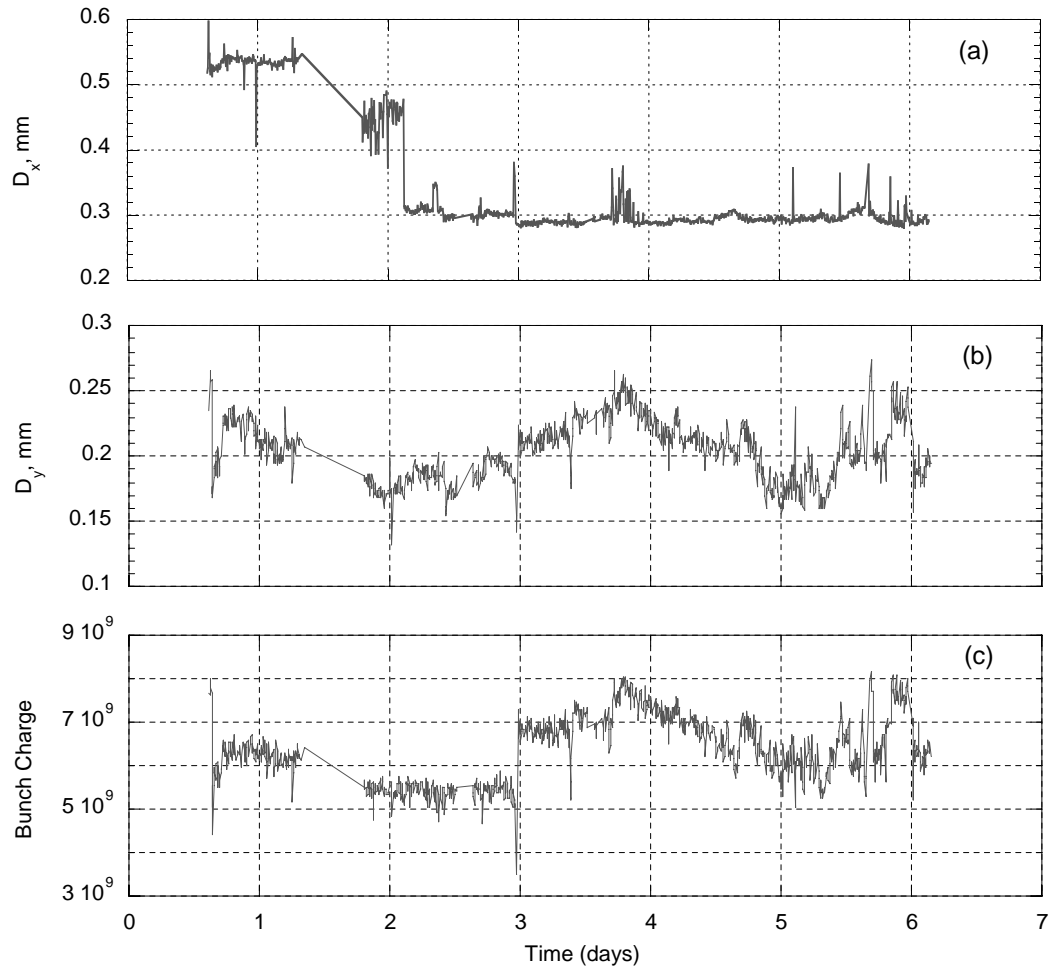


Figure 15.

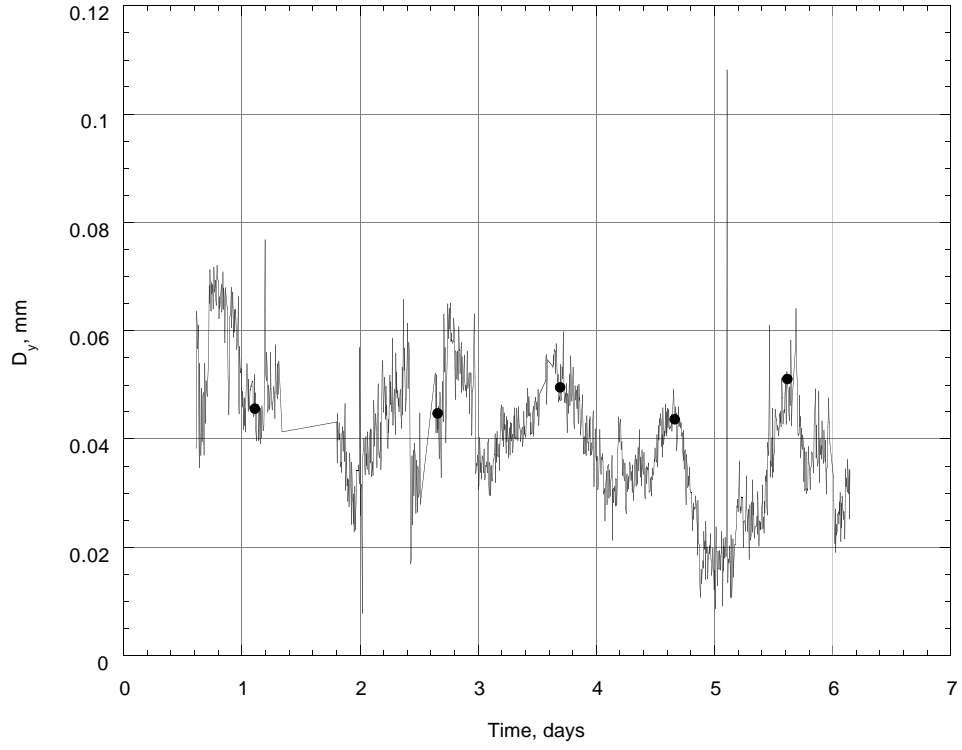


Figure 16.

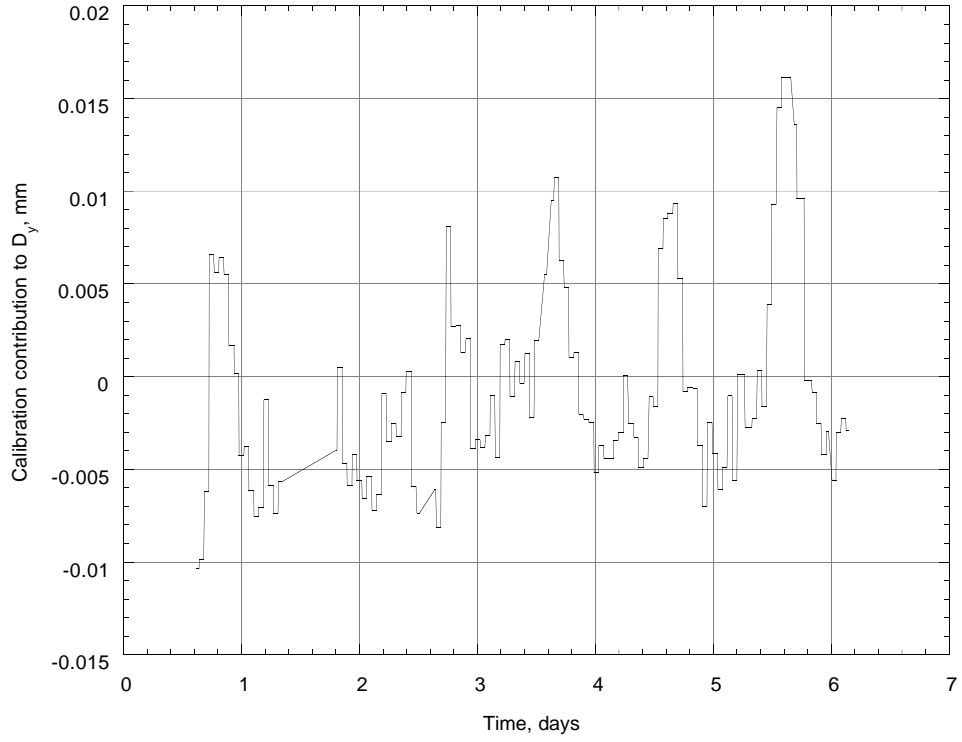


Figure 17.

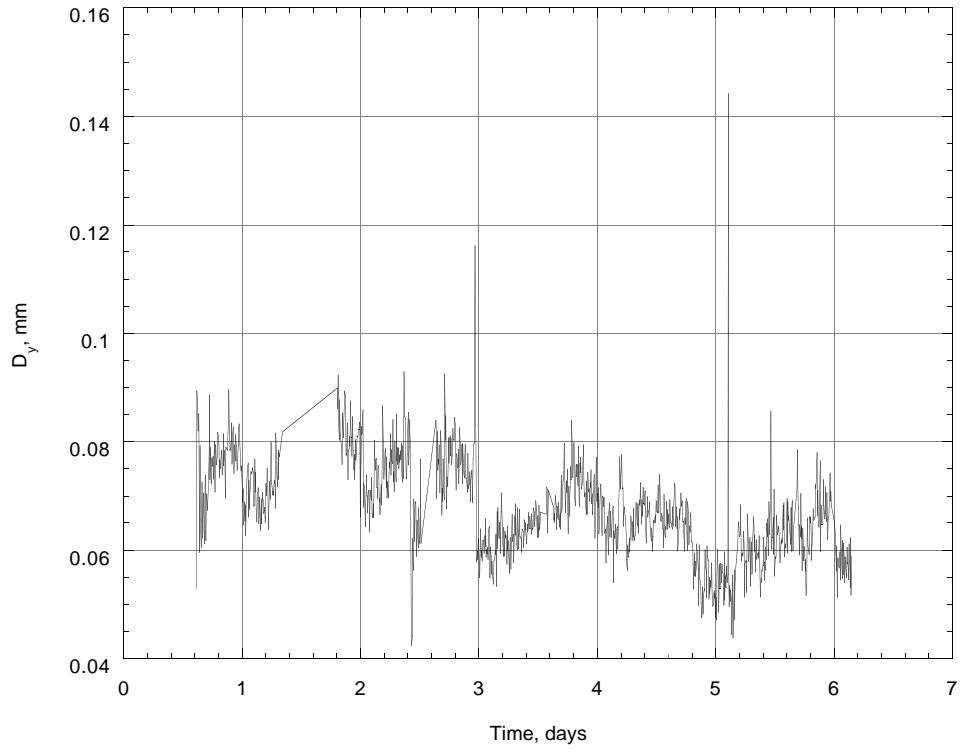


Figure 18.